Temperature Anomalies Between San Francisco and Honolulu, 1966–1974, Gridded by an Objective Analysis

CLIVE E. DORMAN

Department of Geological Sciences, San Diego State University, Calif. 92182

J. F. T. SAUR[1]

Scripps Institution of Oceanography, University of California, San Diego, La Jolla, Calif. 92093

Manuscript received 28 March 1977, in final form 5 December 1977)

ABSTRACT

Over the eight years of expendable bathythermograph observations from merchant ship transits between San Francisco and Honolulu have been analyzed to determine the nature of subsurface temperature anomalies. The irregularly distributed data were interpolated for 0, 90, 170 and 400 m by an objective analysis and then contoured. Statistical properties which had to be computed for the gridding procedure are described and presented.

The statistical properties and anomaly patterns in the upper layers are contrastingly different from those in the main thermocline and below. In the upper layers the significant correlation of anomalies is limited to time separation of less than 40 days, but extends to distance separations beyond 900 km. At the 170 m level in the main thermocline, anomalies are correlated to 100 days, but extend to only 190 km. The standard deviation increases from the surface to 170 m and then decreases to a minimum at 500 m. The peak of the standard deviation at a level shifts west as depth increases. Vertical correlations reveal that temperature anomalies at the surface are uncorrelated with those in the main thermocline. The main thermocline anomalies move along the route toward Honolulu at about 2.9 cm s^{-1}, which is suggestive of baroclinic Rossby waves.

1. Introduction

The western parts of oceans have traditionally received more interest than the eastern. This is probably due to the more intense features in the western areas such as the western boundary currents and, more recently, the discovery of vigorous eddies. However, understanding of the eastern oceanic processes is necessary to make a complete picture of the oceans.

Some studies of temperature anomalies in the surface layers have been made in the eastern North Pacific. Namias (1975) has shown that the lower atmosphere greatly influences the upper ocean thermal structure. Clark (1972) points out a close association between anomalous surface temperature and atmospheric heat transfer and advection due to wind-driven currents. Emery (1975), in a study of temperature anomalies near the San Francisco to Honolulu cross section, noted the independence of the surface and deeper layers. These works show that meteorological processes tend to dominate the surface layers but do not directly affect the deeper layers.

Indications of the complexities of anomalies in the subsurface layers in the central North Pacific have been made by Bernstein and White (1974). They have described the complexities as mesoscale thermal activity with time scales of 100 days and 500 km. They concluded that these mesoscale variations could be baroclinic eddies. Bernstein *et al.* (1977) have documented mesoscale eddy formation in the California Current with satellite observations.

In this study, we examine the nature of temperature anomalies in an extensive series of expendable bathythermograph (XBT) observations on or near the great circle route between Honolulu and San Francisco (Fig. 1). Anomalies of temperature from the mean seasonal cycle were calculated, and their standard deviations and time-space correlations computed. Using these parameters, the temperature anomalies were gridded by an objective analysis program and contoured. Here we present some of the statistical properties of the anomalies and their time-distance distributions along the route at the surface and three characteristic subsurface levels.

2. Background of the area

We briefly review the surface water masses and currents in the eastern North Pacific Ocean. We

[1] Through 1974 with National Marine Fisheries, Southwest Fisheries Center, La Jolla, Calif. 92038.

0022-3670/78/0247-0257$05.50

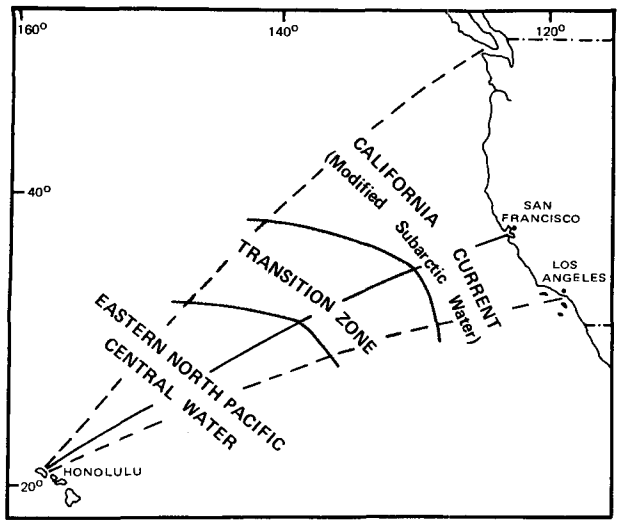

FIG. 1. The great circle route between Honolulu and San Francisco (solid line) where the XBT sections were taken. Surface water masses are shown schematically (after Saur, 1974).

use a system of classification found in Roden (1971, 1975), Lynn and Laurs (1974), Saur (1974) and Laurs and Lynn (1975), given in Fig. 1. The upper ocean waters are divided into three major zones. Cool, low-salinity water occurs off the California coast. This water is of subarctic origin but is modified as it flows southeastward along the coast. Farther to the west is the warm, high-salinity, eastern North Pacific central water. These two water masses are separated by a transition zone which is complex and not fully understood.

The average currents are generally from the northwest at 1–2 n mi day^{-1} (2–4 cm s^{-1}), according to Sverdrup *et al.* (1942), and would be nearly normal to the XBT sections. But the *Climatological and Oceanographic Atlas for Mariners* (U.S. Navy Hydrographic Office, 1961) shows a clockwise current gyre during the summer that extends from Honolulu to half the distance to San Francisco. From oceanographic observations in June of the years 1971–76, Lynn (personal communication) has often found strong but variable filaments of geostrophic current at the boundaries of the transition zone. Otherwise, information regarding detailed current patterns in this part of the eastern North Pacific is minimal.

3. Observations

The time-series of XBT observations analyzed here were collected under the direction of the National Marine Fisheries Service (NMFS). XBT systems were placed on merchant ships sailing between San Francisco and Honolulu. The observations were made by ships' mates (Saur and Stevens, 1972) in deep water between Oahu and the edge of the continental shelf off San Francisco.

The distribution of observations for the period June 1966–December 1974 is shown in Fig. 2. An observation is located by its great circle distance from the reference point (21° 12′N, 157° 42′W) off the southeast tip of Oahu. With a few exceptions, one ship making a round trip every three weeks made all of the observations from June 1966–January 1971. Observations were made about 125 km apart

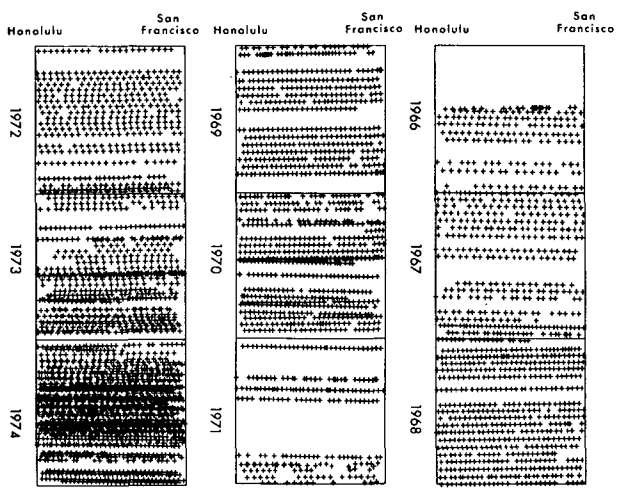

FIG. 2. Distribution of XBT observations at the surface, June 1966–December 1974. Distance on this and other figures is measured by great circle distance from a reference point near Honolulu.

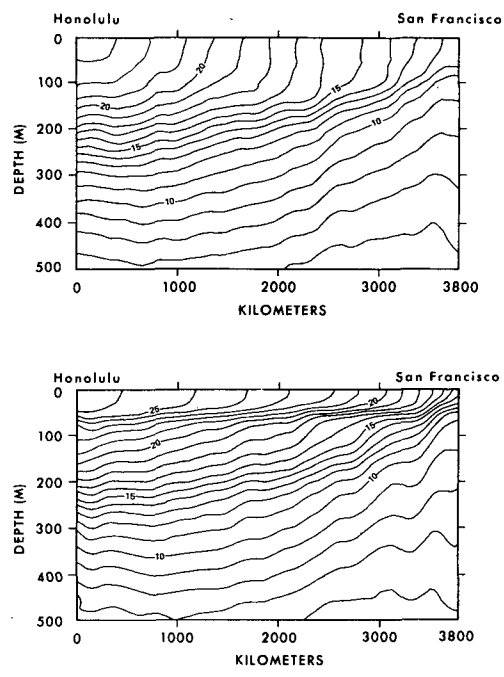

FIG. 3. Vertical sections of mean temperature (°C) for 1 April (upper graph) and mid-September (lower graph).

during transits which took five days one way. Prolonged maritime strikes resulted in a sizable data gap in 1971. In 1972 a faster ship was used which resulted in an observational transit every two weeks, but a spacing between observations of about 160 km. Observations were increased in 1973 by the participation of more ships and intense coverage was obtained in 1974.

Methods for obtaining digitized data varied from automatic recording to subjective reading of analog outputs during the early years of the project, through 1969. Dorman and Saur (1977) and Saur *et al.* (1978) give further details on observations and methods. Observations for 1970 and later were digitized using facilities and computers of the Fleet Numerical Weather Central, Monterey, and following generally the procedures given by Dale and Stevens (1970), but modified by D. R. McLain for NMFS purposes. For all data, preliminary plots of vertical sections were reviewed to eliminate or correct erroneous data and the set of 4899 observations was then compiled for this analysis.

4. The method of objective analysis

The method of an objectively interpolated analysis is used to interpolate temperature anomalies T' from the irregularly placed observations to regular grid points. The coordinates of the grid are distance from Hawaii along the great circle route and time. An elaboration of the theory may be found in Gandin (1963) or Alaka and Elvander (1972).

Briefly, the technique computes the correlations of the temperature anomalies as a function of time and distance separations, t' and x'. The temperature anomalies are paired into time and distance separation groups of $m(\Delta t) \pm \Delta t/2$ and $n(\Delta x) \pm \Delta x/2$. Thus the correlation at group (mn) with L pairs is

$$\mathrm{COR}_{mn} = \Big(\sum_{i,j=1}^{L} T_i' T_j'\Big)\Big(\sum_{i=1}^{L} T_i'^2 \cdot \sum_{j=1}^{L} T_j'^2\Big)^{-1/2}, \quad (1)$$

where i represents the first member of a pair and j the second.

This formula gives correlation as a discrete func-

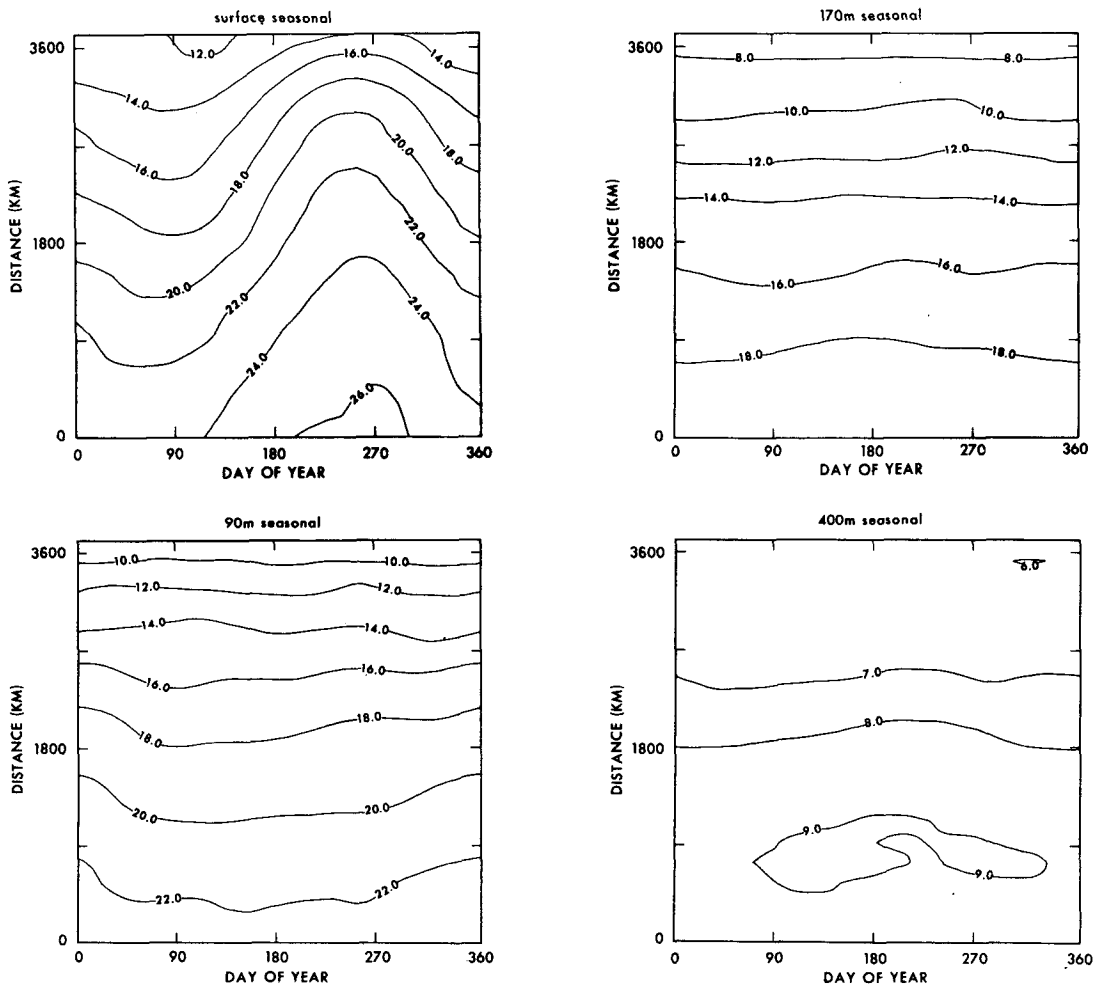

FIG. 4. The mean seasonal variation of temperature (°C) at the surface, 90 m, 170 m and 400 m. Vertical axis is the great circle distance from Honolulu.

tion. Since the objective analysis computer program requires continuous functions we have to take a continuous function of the form

$$C = D \exp(-At - Bx) \quad (2)$$

and fit it to the discrete correlations function just calculated. Here t is the time separation and x is distance separation, both of which are always positive.

This statistical fitting was found to be adequate. A more elaborate fitting of the continuous function to the discrete correlation function does not improve the error due to the nature of this data set. When empirical tests were made by varying the correlation functions and observing the changes in the analysis, major changes in the correlation functions resulted in only minor changes in the objective analysis for this data set. For this reason, the simple formula will be used to perform the objective analysis.

For the objective interpolation of the irregularly distributed anomalies to the grid system, Eq. (2) is utilized to find m temperature anomaly points which have the highest correlation to the grid point P. We selected $m = 8$. The value of the anomaly at P is then

$$T_P' = \sum_{k=1}^{m} \alpha_k T_k', \quad (3)$$

where α are a set of weighting functions which satisfy a set of linear equations

$$\sum_{j=1}^{8} C_{ij}\alpha_j = C_{Pi}. \quad (4)$$

In (4), C_{ij} is the value of the correlations functions

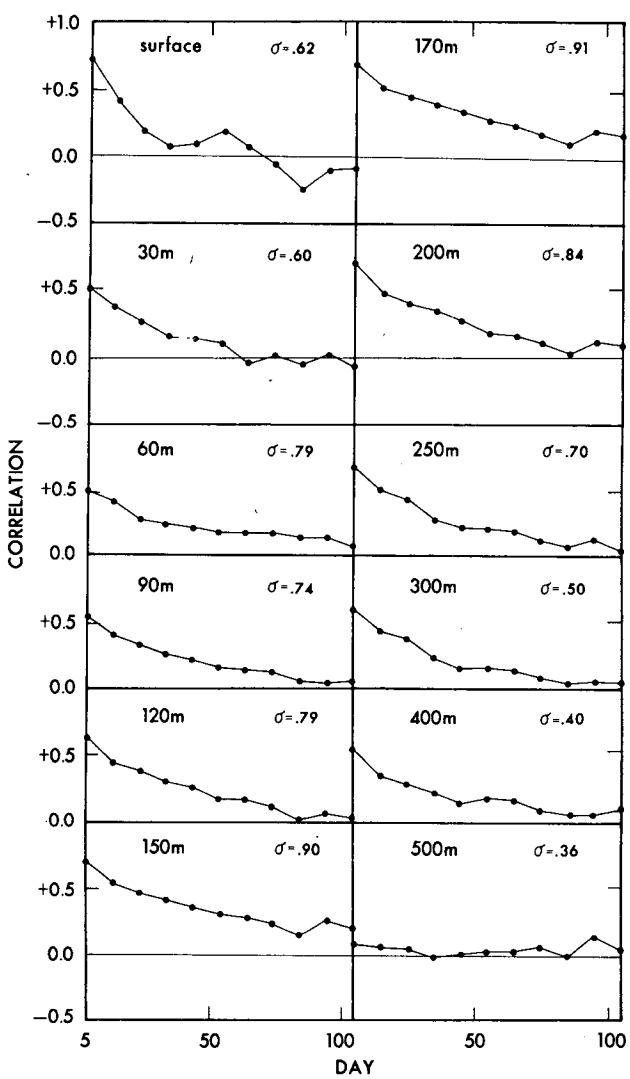

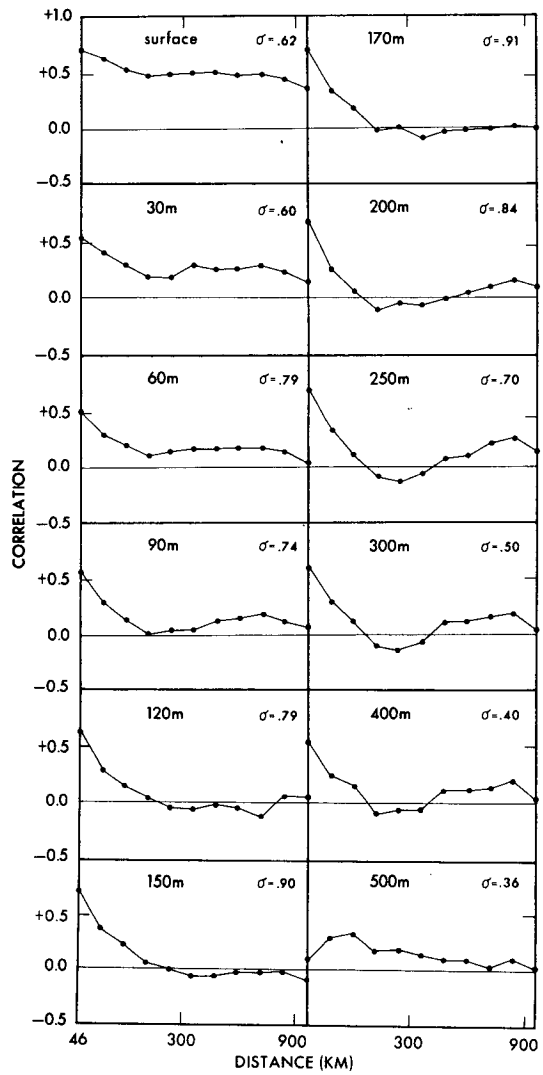

FIG. 5a. Correlations for selected levels as a function of time separation. Distance separation is less than 41 km. The standard deviation in degrees Celsius, for each level, is in the upper right-hand corner of each graph. The 0.95 level of significance is estimated as 0.15.

FIG. 5b. As in Fig. 5a except as a function of distance separation. Time separation is less than 5 days.

between data points i and j ($C_{ij} = 1$ when $i = j$) and C_{Pi} is the value of the correlation function for the time-distance separation between the grid point and data point i.

Contouring of the objectively gridded anomalies is carried out by a routine machine program that finds contour crossings in sub-areas of the array and arrives at a smoothed contour placement. The result is a contoured, objectively gridded temperature anomaly map.

The advantage of the objective analysis is that it takes irregularly spaced anomaly data and systematically arrives at a regular array of values that can be machine contoured. This type of analysis reduces the effect of errors and tends to smooth out the small-scale variability. When there are no data "near" a grid point, the value of the anomaly assigned to the grid approaches zero. Since this type of analysis is well suited to the data we used it to prepare the horizontal maps of temperature anomalies.

5. Mean seasonal variation

Mean seasonal variations based on the 1966–74 period have been derived by Saur *et al.* (1978) using least-squares fits of the first three harmonics of a year at each point in a vertical cross-section grid (92 km by 10 m). Mean vertical sections are shown in Fig. 3 for 1 April and mid-September, respectively, the coolest and warmest times of the year at the surface. On 1 April throughout most of the section there is a deep surface layer in which the isotherms rise abruptly to the surface. On the other hand, by 15 September the summer warming has created a thin, warm surface layer with the seasonal thermocline between 60 and 80 m. Some of the characteristics of standard deviations and correlation functions to be shown may be explained by the fact that the 90 m level is generally in the mixed layer in winter, but at the base of the seasonal thermocline in summer. Over most of the route the 170 m level is in the permanent thermocline throughout the year; and the 400 m level is representative of the region below the main thermocline.

The spatial and seasonal distributions of the mean for depths of 0, 90, 170 and 400 m are shown in Fig. 4. At the surface a seasonal warming and cooling cycle of 3–5°C is superimposed on a temperature field which increases nearly uniformly westward. At 90 m the seasonal warming and cool-

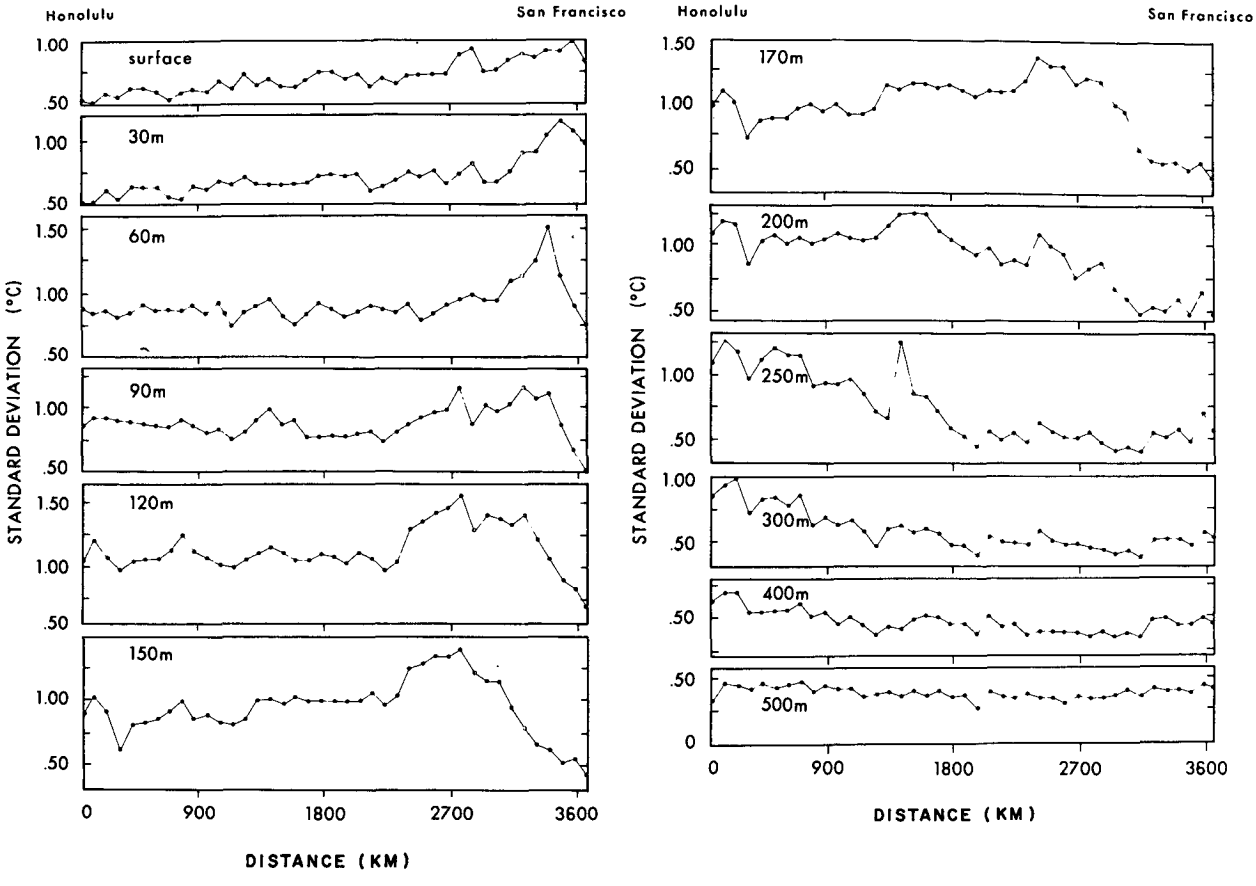

FIG. 6. Standard deviations of temperature anomalies (°C) within a 92 km interval. The change in position of the peak deviation along the route as the depth increases is apparent.

ing effects are small and appear primarily in only the western two-thirds of the route. At 170 m coherent seasonal effects are absent. A westward positive temperature gradient dominates which is slightly stronger in the region of the transition zone between 2000 and 3000 km from Honolulu. At 400 m the range of temperature over the whole route is only a few degrees Celsius and the largest gradient is centered in the area of the subtropical front around 2000 km from Honolulu.

6. Correlation and standard deviation analysis

Temperature anomalies for each observation were obtained by removing the mean seasonal variations just described. The temperature anomaly pairs were correlated from 1974 high density data using the objective analysis method (1). The pairs were grouped by 92 km distance and 10-day time separations. In computing the time and space correlations at selected levels from the surface to 500 m, the minimum number of observational pairs was 1178 at the surface and 950 at 500 m. If the data in each set were independent, the 0.95 level of significance of the correlation coefficients would be 0.08 and 0.09 (Wine, 1964), respectively. However, because they are not independent (Davis, 1976), the 0.95 level of significance is estimated to be approximately 0.15.

Figs. 5a and 5b show the discrete correlations on the time axis and the distance axis, respectively, for selected levels from the surface to 500 m. At the surface the significant time correlation is limited to 30 days, whereas the distance correlation is significant beyond 900 km. The time correlation has a zero crossing around 75 days. In contrast, Roden and Groves (1960) found the surface temperature at 25–30°N, 140–145°W to have a significant correlation of 4 months. But, their longer time correlations are due to longer time averages (monthly) over a large area (5° square) which causes the time correlation to be longer (Munk, 1960).

In contrast to the surface is the 170 m layer. The time correlation at this depth stays weakly positive up to 100 days while the distance correlation is significant only to 250 km. This level has the largest correlation (0.7) of all of the levels within the first 92 km and 10-day separation, and also the largest standard deviation, but the correlation is not significantly larger than any other level between 150 and 250 m. The permanent thermocline is located between these depths over most of the route.

The change in character of the correlations between the surface layers and the permanent thermocline begins around the 90 m level. It is the shallowest level that the distance correlation approaches zero at separations of 250 km. The standard deviation at each level increases from the surface to 60 m,

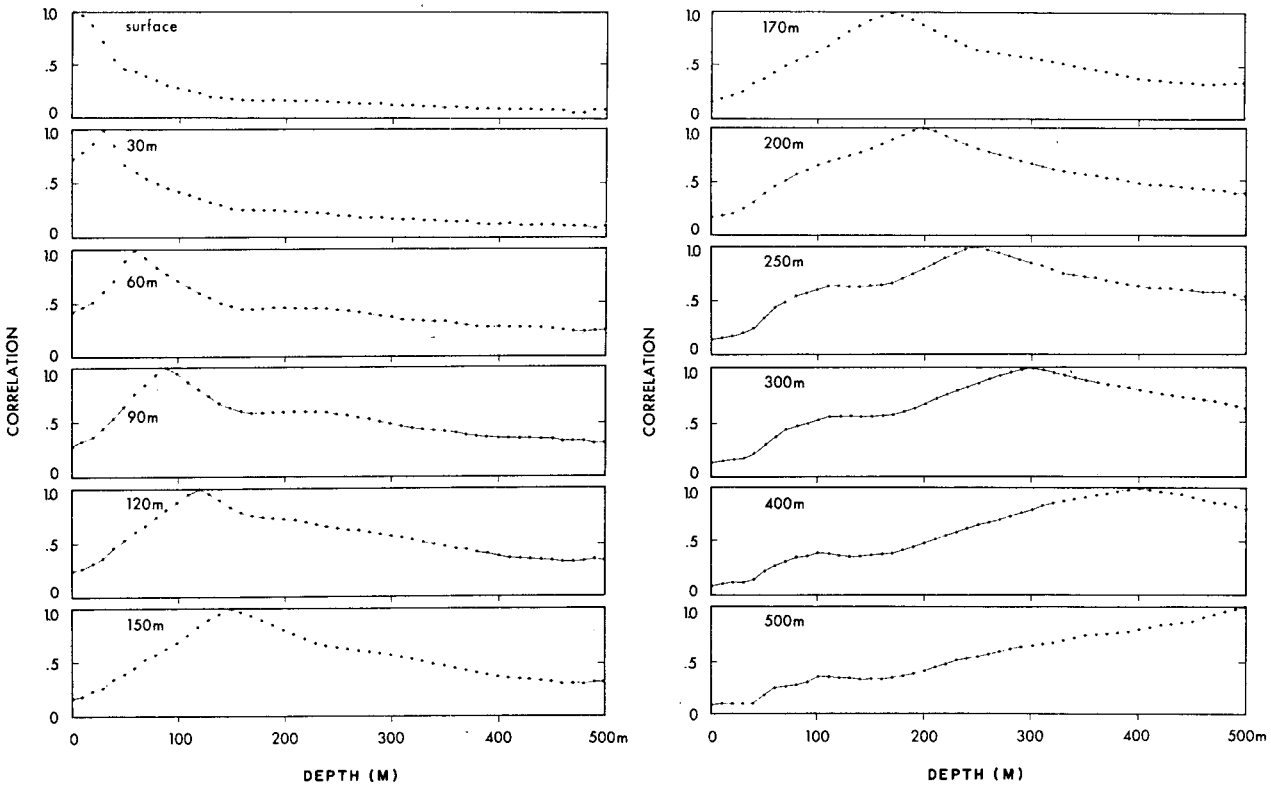

FIG. 7. Vertical correlations of temperature anomalies for all XBTs in 1974.

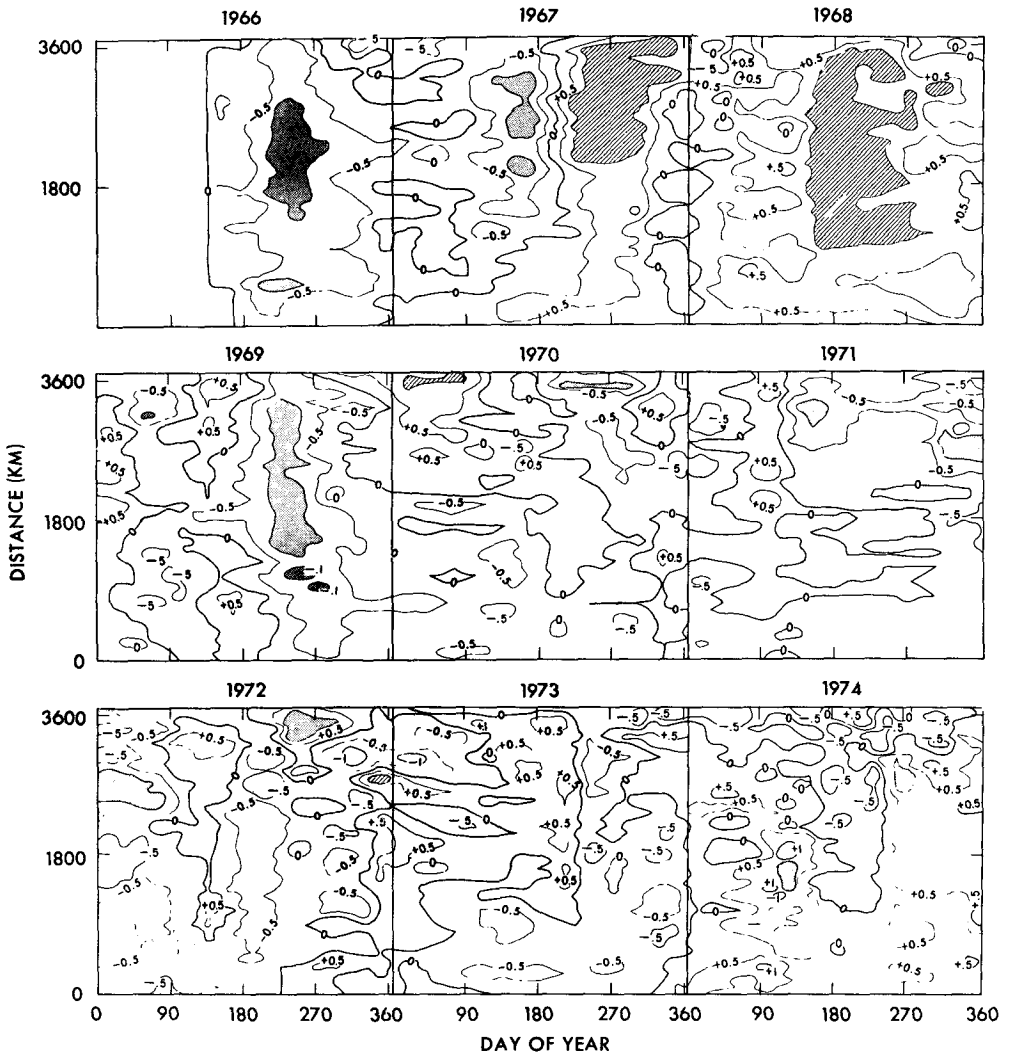

FIG. 8. Objectively gridded surface temperature anomaly patterns, 1966–74. Anomalies below −1.0°C are dark and above 1.0°C are cross-hatched. Contours of greater magnitude are omitted.

is the local minimum at 90 m, and then increases again with depth to 170 m. These changes are caused by the 90 m layer being mostly in the mixed layer in the winter but at the base of the seasonal thermocline in the summer. Below 170 m the shapes of the correlation curves are similar but the correlation magnitudes and standard deviations decrease with increasing depth.

At the 500 m level both the time and distance correlations are very low except for the rather small rise in distance correlations to 0.4 at 92 and 185 km. These indicate that the sampling error (noise) within the first 10-day by 92 km interval is as large as any signals at longer times or greater distances.

Next we shall consider how the temperature standard deviation at selected levels varies with location along the route. A level was divided into 92 km sections and the standard deviation of the temperature anomaly was computed for each section using the high density 1974 data. Fig. 6 shows that the maximum variability moves westward along the track as the depth level increases. The maximum standard deviations in the upper 60 m occur near San Francisco. At 250 m the maximum variability is near the Honolulu end of the route. The shift of maximum variability to the west is associated with the change in depth of the permanent thermocline. Internal gravity waves, baroclinic waves, eddies in the water column and year-to-year changes in geostrophic currents, all contribute to maximum standard deviations in the permanent thermocline. Below 250 m, the peak of the standard deviation for the level decreases to the point that at 500 m there is no maximum at all.

Vertical correlations of temperature anomalies for the 1974 data were also investigated. A particular

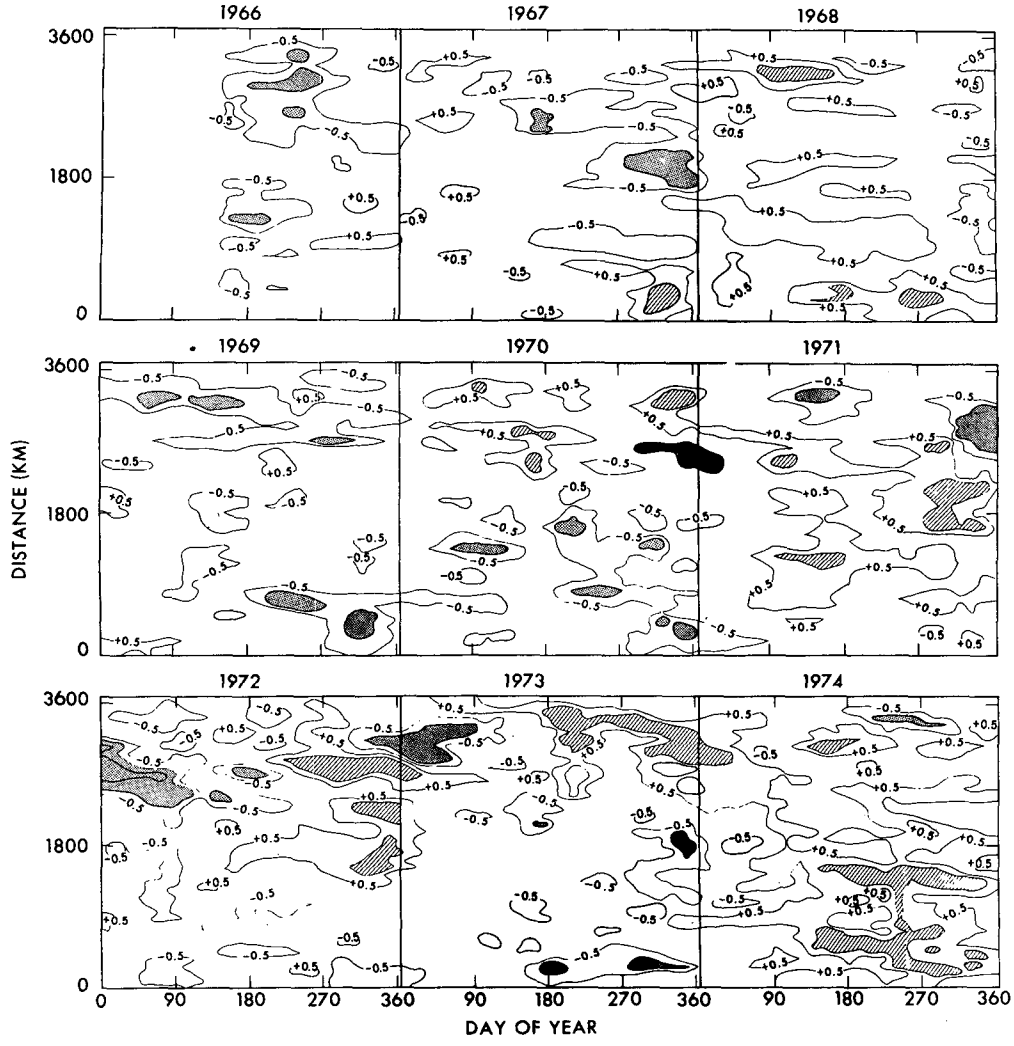

FIG. 9. As in Fig. 8 except for the 90 m temperature anomaly patterns. The 0°C contours are omitted.

level was chosen and the anomaly was paired with the anomaly at another level in the same XBT, and correlations computed for the entire set of 1974 observations. The vertical correlations based at selected levels are displayed in Fig. 7. As one might expect, the correlation with surface anomalies dies out rapidly with increasing depth to 50 m, less rapidly to 120 m, and is low to insignificant for depths below 150 m. Anomalies at 120 m and below tend to be correlated with each other, but not with levels above 50 m. This indicates that we have a two-layer system with the anomalies above 50 m behaving differently than those below 120 m, while the boundary is between 60 and 110 m.

This variation of the correlations and standard deviations is due to the nature of the levels. The deeper levels at 90 m and below are typified by mesoscales. The surface levels are characterized by synoptic scales. These scales are different because of different forcing processes. The broad surface scales are generated by net surface heat fluxes and carried along by the general flow (Namias, 1975; Clark, 1972). The processes which generate mesoscale anomalies at the deeper depths are presently unknown.

7. Temperature anomaly maps

We utilized the objective analysis to grid maps and then contoured time-distance distributions of the temperature anomalies between San Francisco and Honolulu from June 1966 to 1974 for selected levels. The surface, 90, 170 and 400 m levels are displayed in Figs. 8–11. Additional levels and greater details may be seen in Dorman and Saur (1977).

The surface anomaly patterns are shown in Fig. 8. There anomalies are also typical of the upper few tens of meters. The surface is dominated by large-scale features. Most of the anomalies occupy a sig-

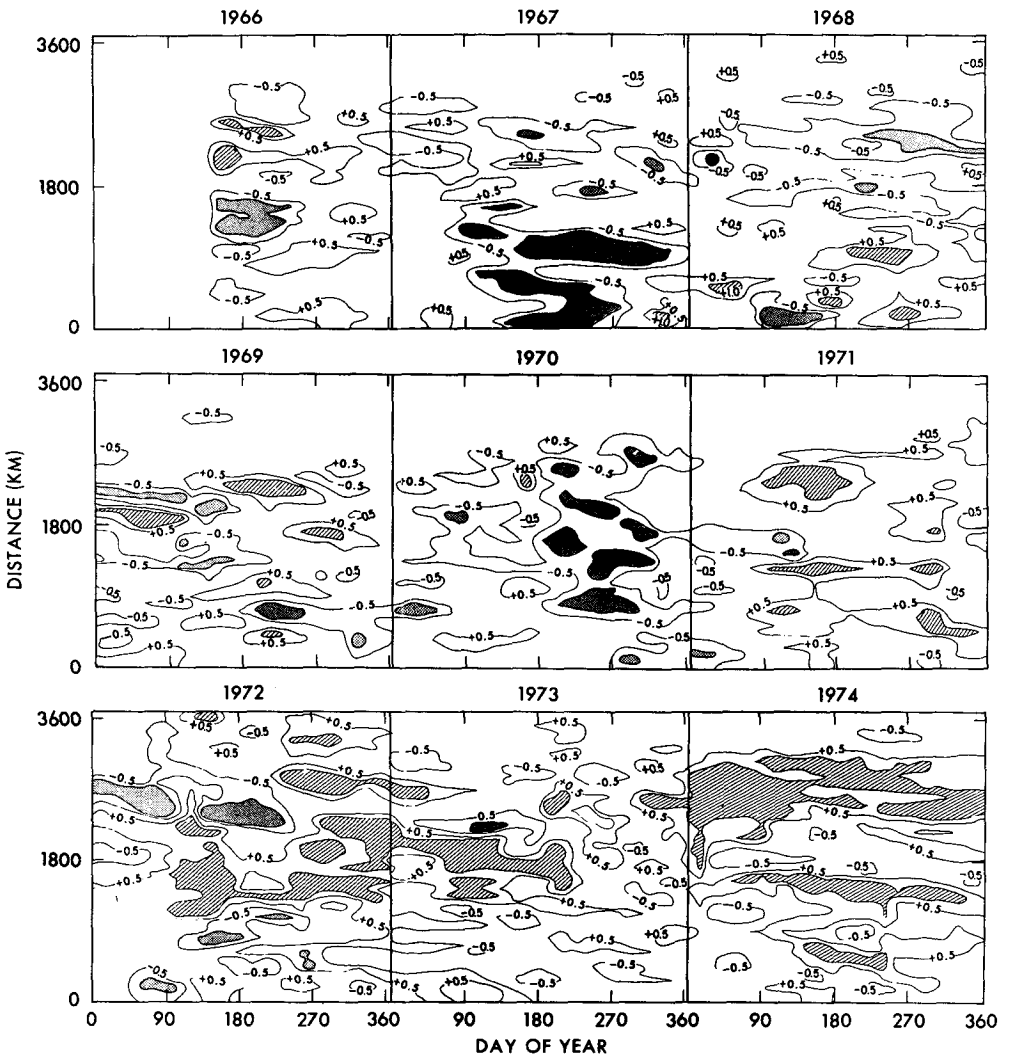

FIG. 10. As in Fig. 8 except for the 170 m temperature anomaly patterns. The 0°C contours are omitted.

nificant portion of the cross section. In 1967, 1973 and 1974 (and, to some extent, 1970) there is a uniform sign change in late summer along the route from San Francisco to three-quarters of the distance to Honolulu. This corresponds to the time when the mixed layer begins to deepen slowly after the summer minimum (see Dorman *et al.*, 1974). In 1971, 1972 and 1974 there is a May sign change along the track which corresponds to the seasonal development of the thermocline. The summer anomalies have the greatest magnitude. During the summer, when the mixed layer is shallowest and has the lowest heat capacity, an anomalous heat flux into the surface will cause a larger temperature anomaly than during other times of the year.

The patterns for 90, 170 and 400 m, seen in Figs. 9–11, reveal that the deep anomalies have a three-dimensional structure. There is a high correspondence of the larger anomaly patterns from 90 to 400 m, as the discussion of vertical correlation would lead us to expect. The maximum anomalies are usually near 170 m. By the 400 m depth, the magnitude of the anomalies is greatly reduced. Careful examination of the larger horizontal patterns reveals a movement to the west at ~900 km year^{-1} (2.9 cm s^{-1}). This is about the speed of baroclinic Rossby waves at these latitudes [detected in this area by Emery and Magaard (1976)], which suggests there may be some association between these anomalies and Rossby waves.

A comparison of the surface and deeper level patterns emphasizes the independence of layers. This was already brought out in the discussion of correlation studies based on one year's data. However, the independence of the layers shown there also appears throughout the 8.5 years of anomaly patterns Figs. 8–11). The correlation studies disclosed the different nature of the two-layer system. The maps

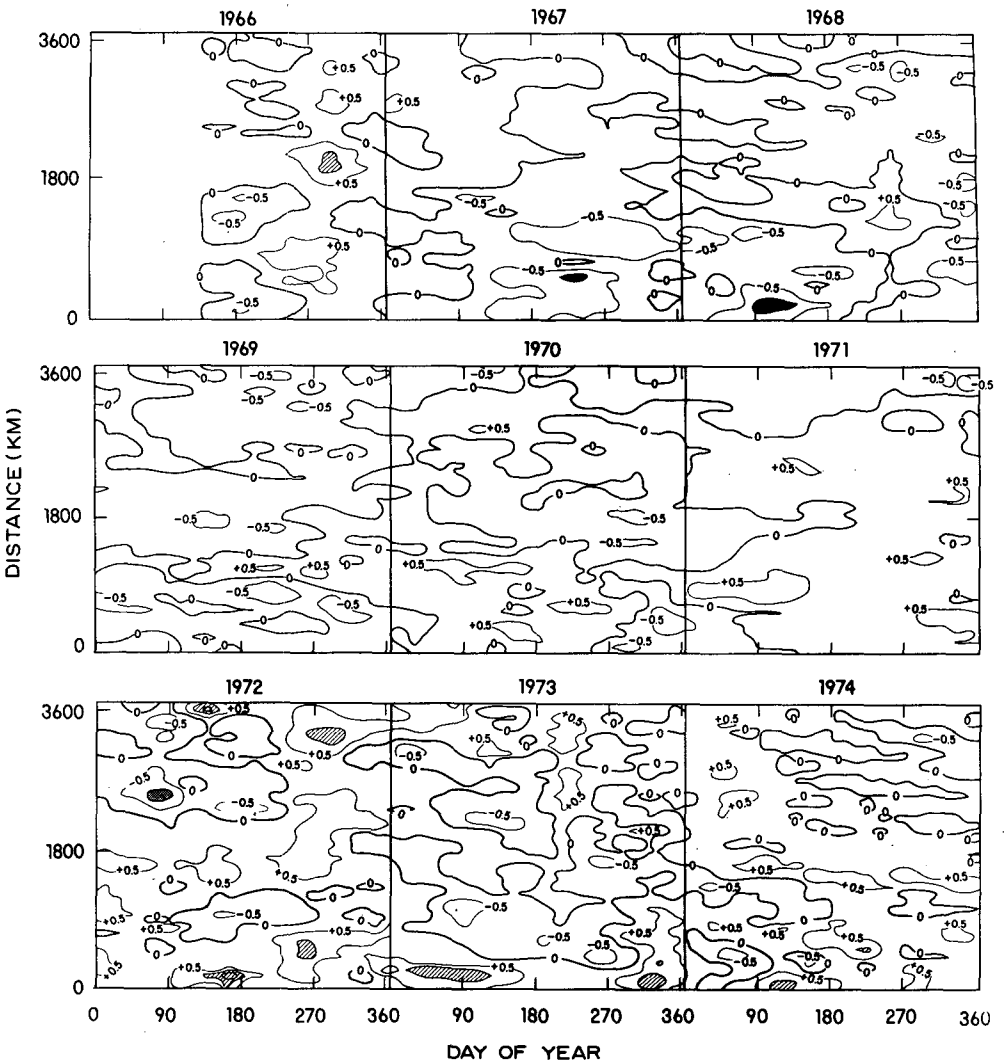

FIG. 11. As in Fig. 8 except for the 400 m temperature anomaly patterns.

underscore this difference. Again we note the surface layers have length scales of synoptic weather patterns, but the deeper layers have mesoscales.

8. Conclusions

In an effort to learn more about temperature anomalies in the northeastern Pacific, we took advantage of unusual XBT data for the great circle route between Honolulu and San Francisco. A particularly efficient way to study the data was by objective analysis. The foundation work for the analysis included various correlation and mean studies. With this background, we gridded horizontal anomaly maps.

One of the results of our analysis was the independence of the surface and deep layers complementing Emery's (1975) earlier discovery. The deep layer has its maximum temperature anomaly variability in the main thermocline. The surface layer has significant positive correlations of 30 days and 900 km. These are typical of the synoptic scales. There were myriad deeper anomalies that had time and distance correlations of 100 days and 250 km. These are characteristic of mesoscales. There is some organized movement to the west at about the same speed as baroclinic Rossby waves.

Acknowledgments. Dr. R. L. Bernstein proposed the use of the NORPAX objective analysis program. The analysis had been programmed primarily by A. M. Tubbs and R. M. Wylie, Jr. We are indebted to them and to Drs. R. E. Davis and W. B. White for suggestions regarding the analysis. In the collection and compilation of the basic data set, we gratefully acknowledge the cooperation of the Matson Navigation Company, the Chevron Shipping Com-

pany and the Pacific Far East Line; we are also grateful for the support of the Fleet Numerical Weather Central, the National Marine Fisheries Service, the National Science Foundation, and the Office of Naval Research, and the contribution of associates of the second author particularly L. E. Eber, A. J. Good, D. R. McLain and Dorothy D. Roll.

This study was conducted under Grants IDO75-22636 and OCE75-23356 from the National Science Foundation, Office for the International Decade of Ocean Exploration.

REFERENCES

Alaka, M. A., and R. C. Elvander, 1972: Optimum interpolation from observations of mixed quality. *Mon. Wea. Rev.*, **100,** 612–624.

Bernstein, R., and W. B. White, 1974: Time and length scales of baroclinic eddies in the central North Pacific Ocean. *J. Phys. Oceanogr.*, **4,** 613–624.

——, L. Breaker and R. Whritner, 1977: California Current eddy formation: ship, air and satellite results. *Science*, **195,** 353–359.

Clark, N. E., 1972: Specification of sea surface temperature anomaly patterns in the eastern North Pacific. *J. Phys. Oceanogr.*, **2,** 391–404.

Dale, Dean H., and Paul D. Stevens, 1970: Computer processing of expendable bathythermograph traces. Tech. Note 61, U.S. Fleet Numerical Weather Central, 12 pp.

Davis, R. E., 1976: Predictability of sea surface temperature and sea level pressure anomalies over the North Pacific Ocean. *J. Phys. Oceanogr.*, **6,** 249–266.

Dorman, C. E., C. A. Paulson and W. H. Quinn, 1974: An analysis of 20 years of meteorological and oceanographic data from Ocean Station N. *J. Phys Oceanogr.*, **4,** 645–653.

——, and J. F. T. Saur, 1977: Maps of temperature anomalies between San Francisco and Honolulu, 1966–1974, computed by an objective analysis. Center for Marine Studies, San Diego State University, 14 pp.

Emery,W. J., 1975: The role of vertical motion in the heat budget of the upper ocean. HIG-75-3, Hawaii Institute of Geophysics, 81 pp.

——, and L. Magaard, 1976: Baroclinic Rossby waves as inferred from temperature fluctuations in the eastern Pacific. *J. Mar. Res.*, **34,** 365–385.

Gandin, L. S., 1963: Objective analysis of meteorological fields. NTIS-translation TT-65-50007, 242 pp.

Laurs, R. M., and R. J. Lynn, 1975: The association of ocean boundary features and albacore tuna in the northeast Pacific. *Proc. Third S/T/D Conference and Workshop*, San Diego, Plessy, Inc., 23–30.

Lynn, R. J., and R. M. Laurs, 1974: Cooperative NMFS-AFRF early season offshore studies conducted during 1974. Southwest Fisheries Center Admin. Rep. LJ-74-47, 3–18.

Munk, W. H., 1960: Smoothing and persistence. *J. Meteor.*, **17,** 91–92.

Namias, J., 1975: Short period climatic variations. *Collected works of J. Namias, 1934–1974*, Vols. I and II, University of California Press, San Diego, 905 pp.

Roden, G. I., 1971: Aspects of the transition zone in the northeastern pacific. *J. Geophys. Res.*, **76,** 3462–3475.

——, 1975: On North Pacific temperature, salinity, sound velocity, and density fronts and their relation to the wind and energy flux fields. *J. Phys. Oceanogr.*, **5,** 557–571.

——, and G. W. Groves, 1960: On the statistical prediction of ocean temperatures. *J. Geophys. Res.*, **65,** 249–263.

Saur, J. F. T., 1974: Subsurface temperature structure in the northeast Pacific Ocean. *Fishing Information*, N. 8, NOAA, Nat. Mar. Fish. Serv., SW Fish. Ctr., La Jolla, 3 pp.

——, L. E. Eber, D. R. McLain and C. E. Dorman, 1978: Vertical sections of mean temperature on the San Francisco-Honolulu route: From expendable bathythermograph observations, June 1966–December 1974. NOAA Tech. Rep. (in preparation).

——, and Paul D. Stevens, 1972: Expendable bathythermograph observations from ships of opportunity. *Mar. Wea. Log*, **16,** 1–8.

Sverdrup, H. V., M. W. Johnson and R. H. Fleming, 1942: *The Oceans: Their Chemistry, Physics and General Biology*. Prentice-Hall, 1087 pp.

U.S. Navy Hydrographic Office, 1961: *Climatological and Oceanographic Atlas for Mariners*, Vol. II. *North Pacific Ocean*, Washington, D.C.

Wine, R. L., 1964: *Statistics for Scientists and Engineers*. Prentice-Hall, 671 pp.